Seismic Hazard Along the Southern Coast of Ecuador

Ivan Wong, Mark Dober, Mark Hemphill-Haley & Fabia Terra
URS Corporation, Seismic Hazards Group, Oakland, California, USA

SUMMARY
The coast of Ecuador is situated on the seismically active South America subduction zone. One of the largest earthquakes recorded, the 1906 **M** 8.8 earthquake, occurred along the megathrust beneath coastal Ecuador. We have performed a probabilistic seismic hazard analysis (PSHA) of four cities along the Ecuadorian coast including Guayaquil. Significant uncertainties exist in the characterization of seismic sources and ground motions in Ecuador due to insufficient research and data. These uncertainties have been incorporated into the PSHA. The seismic sources considered include crustal faults, background crustal seismicity and the South America subduction zone, which includes both the megathrust and the Wadati-Benioff zone. Limited paleoseismic data suggests that the crustal faults may have slip rates on the order of 1 to 5 mm/yr or greater. Maximum magnitudes exceed **M** 6.5 based on fault length estimates. Active crustal faults such as the Colonche fault, are significant to the hazard for populated areas such as Guayaquil. State-of-the-art ground motion prediction models for crustal earthquakes in tectonically active regions and worldwide data-derived subduction zone relationships were used. Based on the PSHA, peak horizontal accelerations at a return period of 2,475 years generally exceed 0.6 g for generic soil site conditions. The major contributors to the PGA hazard along the coast are the crustal faults and background earthquakes and the subduction zone megathrust and intraslab seismicity at longer spectral periods (> 1.0 sec).

Keywords: Ecuador, probabilistic seismic hazard, South America subduction zone

1. INTRODUCTION

We have evaluated the seismic hazards along the coast of southern Ecuador by performing a probabilistic seismic hazard analysis (PSHA) for four major coastal cities. The southern Ecuadorian coast is located on the very seismically active North Andean block of the South America subduction zone (Figure 1). The region has been and will be subjected to future strong ground shaking generated by large earthquakes on numerous seismic sources in the region. One of the largest earthquakes ever recorded, moment magnitude (**M**) 8.8, occurred in 1906 along the megathrust of the South America subduction zone (Figure 2).

The primary objective of this study is to estimate the future levels of ground motions along the southern Ecuadorian coast that will be exceeded at specified probabilities. Available geologic and seismologic data have been used to evaluate and characterize potential seismic sources, the likelihood of earthquakes of various magnitudes occurring on those sources, and the likelihood of the earthquakes producing ground motions over a specified level. It should be noted that there are very significant uncertainties in the characterization of seismic sources and ground motions in Ecuador due to lack of sufficient research and these uncertainties have been incorporated into the PSHA. Unlike most studies performed previously for the South America subduction zone, we characterized discrete seismic sources including the megathrust and crustal faults based on paleoseismic and historical seismicity information rather than just using an outdated seismic zonation approach based on historical seismicity data.

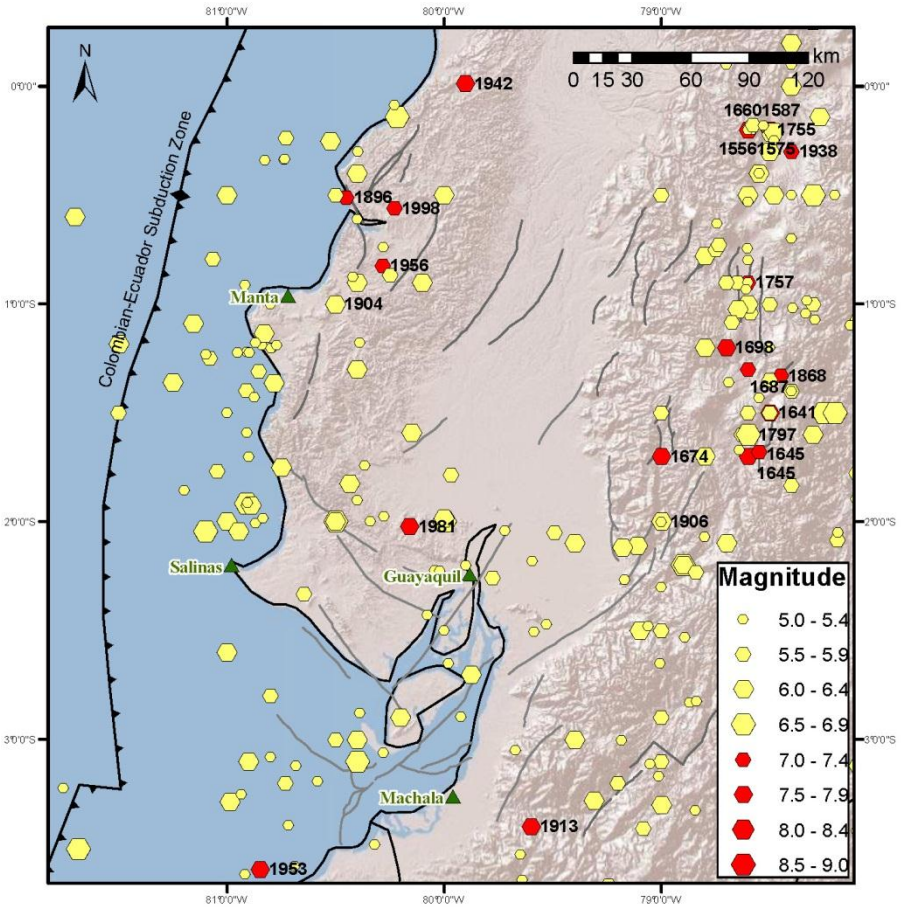

Figure 1. Historical seismicity (**M** ≥ 5.0) in southern Ecuador, 1556 to 2011

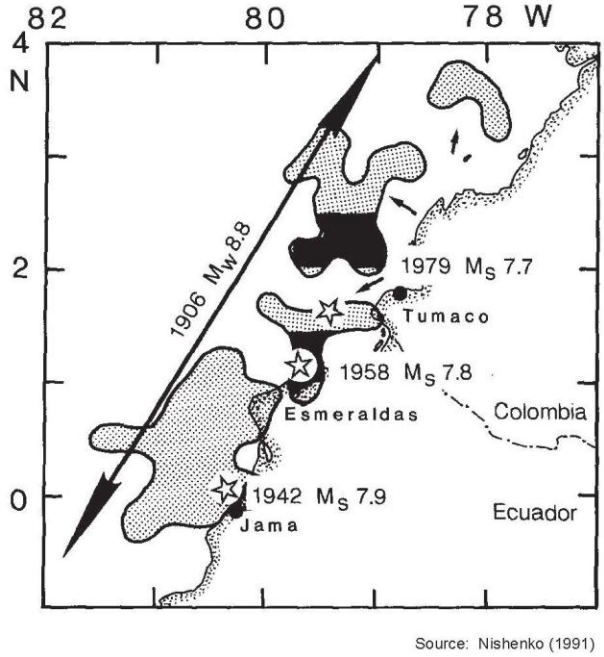

Figure 2. 1906, 1942, 1958, and 1979 Ecuador-Colombia earthquakes

2. SEISMOTECTONIC SETTING AND HISTORICAL SEISMICITY

The coast of southern Ecuador on the South America plate overrides the actively subducting Nazca plate (Figure 1). The South America subduction zone has been the source of some of the largest earthquakes in the world including the largest event known, the 1960 **M** 9.5 Chile earthquake and the 1906 **M** 8.8 Ecuador event (Figure 2). In addition to great earthquakes occurring along the megathrust, seismicity occurring in the crust of South America and within the Nazca plate (Wadati-Benioff zone) has been abundant (Figure 1).

Gutscher *et al.* (1999) have divided the North Andean block of the subduction zone beneath the coasts of Colombia, Ecuador, and northern Peru into four regions based on seismicity, structure, and volcanic characteristics: Region 1 (6°N to 2.5°N) steep east-southeast dipping subduction to a depth of about 200 km and a narrow volcanic arc; Region 2 (2.5°N to 1°S) probable flat slab subduction of the continuation of the Carnegie Ridge, intermediate-depth seismic gap, and a broad volcanic arc; Region 3 (1°S to 2°N) steep northeast-dipping subduction and a narrow volcanic arc; and Region 4 (north of 2°N) flat subduction and no modern volcanic arc. Segments of steep slab subduction alternate with aseismic regions and segments of flat subduction (Gutscher *et al.*, 1999). The collision of the Carnegie Ridge in the past 2 Ma plays a prominent role in the structural and deformational characteristics of the North Andean block of the subduction zone and accounts for the segmentation.

The sources of seismicity in Ecuador include shallow crustal faults, both known and unknown, at depths of less than 30 to 40 km and the South America subduction zone megathrust, and Wadati-Benioff (intraslab) zone. The latter represents the seismicity due to internal deformation primarily from bending of the Nazca plate as it subducts.

A historical earthquake catalogue was compiled for southern Ecuador (Figure 1). The catalog contains more than 3,200 earthquakes spanning the time period from 1556 to 2011. A total of 49 earthquakes larger than or equal to approximately **M** 7 (or MM intensity IX) have been recorded and thought to have occurred in southern Ecuador and vicinity (Figure 1). Five earthquakes are thought to be **M** 8 and greater. The most significant events occurred in 1797 (**M** 8.3), 1901 (**M** 7.8), 1906 (**M** 8.8), 1942 (**M** 7.6), 1958 (**M** 7.7), and 1979 (**M** 8.2) (Figures 1 to 3). The 1906 earthquake ruptured about 500 km of the megathrust and was subsequently followed by events in 1942, 1958, and 1979, which appeared to re-rupture the same portion of the subduction zone (Mendoza and Dewey, 1984) (Figure 2). It should be noted that the 1906 earthquake generated a large tsunami along the coast of Ecuador. All these events appeared to have been megathrust events. A large number of intraslab earthquakes have also struck the country as shown in the space-time plot of the historical record of major earthquakes in Ecuador (Figure 3).

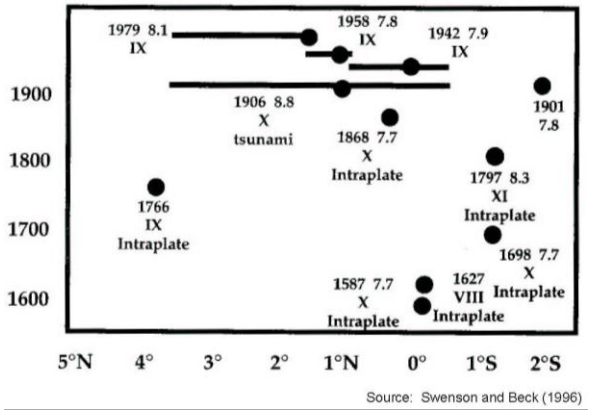

Figure 3. Space-time plot of the northern Ecuador/southern Colombian subduction zone

3. PSHA METHODOLOGY

The PSHA approach used in this study is based on the model developed principally by Cornell (1968). The occurrence of ground motions at the site in excess of a specified level is a Poisson process, if (1) the occurrence of earthquakes is a Poisson process, and (2) the probability that any one event will result in ground motions at the site in excess of a specified level is independent of the occurrence of other events.

For input into the PSHA, seismic sources need to be defined and ground motion prediction models selected. Two types of earthquake sources are characterized in this PSHA: (1) fault sources; and (2) areal source zones. Fault sources are modeled as three-dimensional fault surfaces and details of their behavior are incorporated into the source characterization. Areal source zones are regions where earthquakes are assumed to occur randomly. Seismic sources are modeled in the PSHA in terms of geometry and earthquake recurrence. Uncertainties in the seismic source parameters, which were sometimes large, were incorporated into the PSHA using a logic tree approach. For the ground motion prediction models, we used global relationships for crustal and subduction zone earthquakes.

4. SEISMIC SOURCE CHARACTERIZATION

Seismic source characterization is concerned with three fundamental elements: (1) the identification, location, and geometry of significant sources of earthquakes, (2) the maximum size of the earthquakes associated with these sources, and (3) the rate at which they occur.

4.1. Crustal Faults

Potentially significant active faults within southern Ecuador were identified and assessed through review of existing literature and data. All the faults considered are “active” or “potentially active.” The structures include all Quaternary faults as well as more distant faults capable of producing large magnitude earthquakes and significant ground shaking.

Consistent with current state-of-the-practice, we estimated the maximum magnitudes for the crustal faults based on empirical relations between fault rupture length and/or rupture area and magnitude developed by Wells and Coppersmith (1994). However, considerable uncertainty often exists in the selection of the appropriate rupture length to be used in the analysis. In almost all cases, we have assumed no fault segmentation and that the whole length of the fault could rupture. Fault activity is expressed as an annual average slip rate (in mm/yr) rather than an interseismic interval. The uncertainty in the slip rates, which can be considerable, and the other input parameters uncertainties are accommodated in the PSHA through the use of logic trees.

In the PSHA we have evaluated 16 faults or fault zones within coastal southern Ecuador (Figure 4). Faults basically fall into two groups. Within eastern and southeastern Ecuador are north-northeast-striking faults that are likely a part of the Delores-Guayaquil megashear. These faults display primarily dextral strike-slip motion. They include such faults as the Zambapala-Lechuza fault zone, Puna-Pallatanga fault zone, Naranjal fault, Rîo Colimes fault, Montalvo fault, and Calabî fault (Figure 4).

The second group of faults occurs primarily within central and southern Ecuador (Figure 4). These faults, oriented to the northwest and west-northwest, have been not been studied to the extent that the northeast-striking faults have but have variously been attributed to have normal, reverse and lateral motion likely associated with the opening of the Gulf of Guayaquil as the North Andean block moves to the north-northeast. This group of faults includes the Colonche fault zone, Carrizal fault, La Cruz fault, Chanduy

fault, Chillanes fault, Jambeli fault, Ponce Enriquez fault, Posorja fault, Piqueros fault and Tenguel fault (Figure 4).

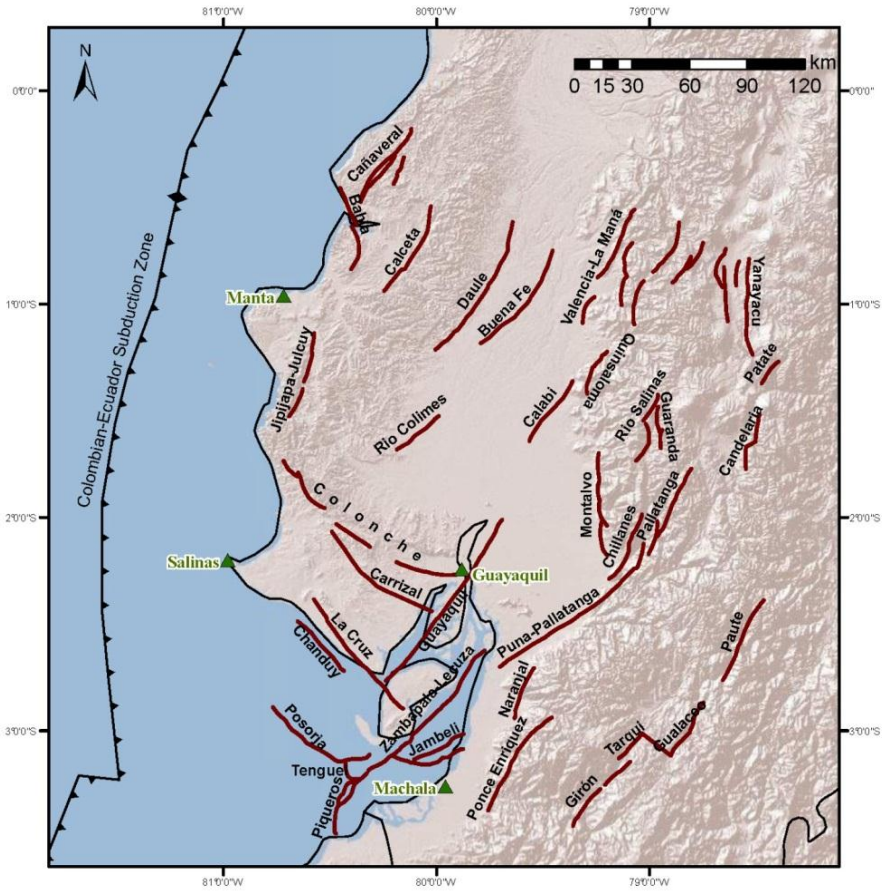

Figure 4. Active and potentially active faults in southern Ecuador

There has been little detailed work conducted to assess the paleoseismic history of most of the faults located in southern Ecuador, with the exception of work by Winter *et al*. (1993), Dumont *et al.* (2005) and Witt *et al*. (2005). The most extensive compilation of the knowledge of most of the faults within Ecuador, provided by Eguez *et al*. (2003), illustrates the need for more comprehensive analyses of the faults.

The Eguez *et al*. (2003) Quaternary fault database includes all faults that were used in the PSHA. In lieu of detailed paleoseismic information to provide data regarding the occurrence of the last surface rupturing earthquake, the recurrence intervals for surface faulting earthquakes or detailed along-fault seismicity, we assumed that faults that are proximal to known active faults, aligned quasi-parallel to known active faults or that appear to have associated seismicity are active.

The range of slip rates that we assessed for faults is intended to span the distribution of possible rates for any given fault. In the case of many of the faults in Ecuador there is little actual slip rate information that has been compiled for any individual fault. However, it appears that much of the structure within the region not directly attributed to the subduction zone is related to the northeast trajectory of the North Andean block. As stated above, we assume that faults either accommodate dextral strike-slip motion associated with the eastern margin of the block or represent deformation within the pull-apart basin along the southern margin of the block. The velocity of the North Andean block is well-constrained primarily

from geodetic studies at about 1 cm/yr (Gutscher *et al*., 1999; Witt *et al*., 2005). The block-like behavior of the Northern Andes is suggested by the concentration of faults along its margins. Thus it seems reasonable that the deformation rates related to its motion are distributed across these faults. The cumulative slip of the north-northeast-striking group of faults must be approximately 1 cm/yr in a dextral sense. Likewise, faults within the southern margin of the North Andean block should accommodate up to 1 cm/yr of its north-northeastward escape. There is uncertainty in the amount of total opening that might occur within the pull-apart structure due to folding and distributed subsidence. Other faults considered in the PSHA have been compiled on the basis of their associations with other, better-studied faults or from information gathered from the Quaternary fault and fold database (Eguez *et al*., 2003).

4.2 Subduction Zone

Megathrust
We model the megathrust based on the historical record (Figures 1 to 3). The portion of the South America subduction zone underlying southern Ecuador consists of two potential segments: the northern Ecuador/southern Colombia segment that ruptured as a whole in 1906 and in partial ruptures in 1942, 1958, and 1979 (Figures 2 and 3) and the southern Ecuador/northern Peru segment. The maximum magnitudes for each segment are shown in Table 1 estimated in large part from the historical record.

Table 1. Ecuador Subduction Zone Megathrust

Segment Name	Latitudinal Extent	Dip	Maximum Depth (km)	Mmax	Recurrence Interval	Recurrence Model
Northern Ecuador/ Southern Colombia	0.5°S – 4.0°N	15 ± 5°	35 ± 5	8.8 ± 0.2	400 (0.3) 800 (0.4) 1,000 (0.3)	Characteristic (0.8) Max Magnitude (0.2)
Southern Ecuador/ Northern Peru	10.8°S – 0.5°S	10° (0.5) 15° (0.5)	30 ± 10	8.0 ± 0.5	400 (0.2) 1,350 (0.6) 10,000 (0.2)	Characteristic (0.8) Max Magnitude (0.2)

The northern Ecuador/southern Colombia segment is assigned a maximum earthquake of **M** 8.8 based on the 1906 earthquake. No megathrust earthquakes are known to have ruptured the segment prior to 1906 and so there has been nearly 400 years between the penultimate event and 1906 earthquake (Figure 3). We adopt recurrence intervals of 400, 800, and 1,000 years (Table 1). The northern Ecuador/southern Colombia segment megathrust is characterized as a planar fault dipping 15° with an uncertainty of ± 5°. The megathrust extends down to a depth of 30 ± 5 km based on observed seismicity. Because the segment has ruptured in smaller events, e.g., 1942, we assign a weight of 0.8 to the characteristic recurrence model (Table 1).

The largest earthquake to possibly rupture the 900-km-long southern Ecuador/northern Peru segment was the 1619 Trujillo earthquake of estimated **M** 7.7 to 8. The observation that no tsunami was generated raises doubt on whether the event occurred on the megathrust. Two smaller earthquakes in 1960 and 1996 (**M** < 8) occurred on the megathrust. This portion of the South America subduction zone undergoes flat subduction and its potential for generating great earthquakes (**M** ≥ 8.0) is poorly understood. Both Pelayo and Wiens (1990) and Bourgeois *et al*. (1999) conclude that the subduction zone beneath northern Peru is weakly coupled and that convergence is largely aseismic based on examinations of the 1960 and 1996 (**M** < 8) earthquakes and their tsunamis.

It is unlikely that the whole segment could rupture in a single great earthquake. We assign a Mmax distribution of **M** 8.0 ± 0.5. The plate dips at an angle of about 10° ± 5°, which we used to define the

approximate eastern boundary of the rupture zone. This portrayal generally agrees with the contemporary seismicity. The maximum depth of the seismogenic megathrust is uncertain. We model the geometry so the maximum depth reaches 30 ± 10 km. The value of 40 km is a typical maximum depth for many subduction zones (Ruff and Kanamori, 1983).

Subduction of the "massive" Carnegie Ridge complex could lead to greater than average recurrence intervals (Nishenko, 1991). Based on the observation that no megathrust earthquake of **M** ≥ 8.0 has been observed along this segment in nearly 400 years with the possible exception of the 1619 event, we adopt recurrence intervals of 400, 1,350, and 10,000 years (Table 1). The best estimate value of 1,350 years is the mean recurrence interval from Bourgois *et al*. (2007). The very long interval of 10,000 years roughly equivalent to the Holocene period is to acknowledge the observation that **M** ≥ 8.0 events are unlikely.

Intraslab Seismicity
Based on the 1970 **M** 7.9 event, intraslab earthquakes within the subducting plate are assumed to have a maximum magnitude of **M** 7.75 ± 0.25. We have modeled the Wadati-Benioff zone as three zones (northern, central, and southern) beneath Ecuador based on the regionalization of Gutscher *et al*. (1999). We model the intraslab zones as a series of staircasing blocks of varying width depending on the along-strike length of the zone and 15 km thick to approximate the dipping Nazca plate. The closest approach of the Nazca plate to the coast is at an approximate distance of 50 ± 10 km.

In order to estimate probabilistic ground motions, earthquake recurrence parameters are required for the intraslab events within the subducting Nazca plate and for the "background" seismicity occurring within the South American crust. The recurrence rates for the intraslab earthquakes were based on the following analysis.

Only earthquakes in the historical catalog dating back to 1962 were used in the recurrence estimates. Prior to this time, seismographic coverage was sparse for South America and so the historical record was very incomplete. Intraslab earthquakes in the catalog were identified based on the geometry of the subduction zone. The recurrence relationships were estimated following the maximum likelihood procedure developed by Weichert (1980) and estimated completeness intervals for the region. Dependent events and foreshocks and aftershocks were identified using empirical criteria for the size in time and space of foreshock-mainshock-aftershock sequences. The resulting catalog for independent events was then used to develop the recurrence relationships. Regression was performed on the resulting data points as described in Weichert (1980). The calculated recurrence for **M** 7 and greater earthquakes in the southern Ecuador intraslab zone is 53 years.

4.3 Crustal Background Seismicity

Background or random earthquakes are those events, which can occur without an apparent association with a known or identified tectonic feature. Within the southern Ecuador crust, seismicity is distributed diffusely with no clear relationships with any geologic structures. The hazard from such sources is incorporated into the PSHA through an areal source zone.

We divided southern Ecuador into two seismotectonic provinces, the coastal zone and the Andes zone. We estimate the maximum magnitude for the background earthquake to be between **M** 7.0 and 7.5. Earthquakes larger than **M** 6.5 to 7.0 will typically be accompanied by surface rupture and thus repeated events of this size will produce recognizable fault-related geomorphic features at the earthquake's surface. However, the higher magnitudes of **M** 7.0 to 7.5 reflect the fact that crustal faults in Ecuador and Peru have received little attention and undoubtedly there are active faults that have not been identified and

included in the PSHA. The recurrence for the crustal "background" seismicity was computed in the same manner as for the intraslab zones.

5. GROUND MOTION PREDICTION MODELS

The traditional approach for estimating ground motions in seismic hazard analysis utilizes empirical ground motion prediction models, which are derived from strong motion data. Because few strong motion records exist in Ecuador, we know of no crustal or subduction zone ground motion prediction models that are specific to the country. Thus, in this evaluation, the Pacific Earthquake Engineering Research (PEER) Next Generation of Attenuation (NGA) ground motion prediction models for tectonically active regions were used: Abrahamson and Silva (2008), Chiou and Youngs (2008), Campbell and Bozorgnia (2008), and Boore and Atkinson (2008).

Arango *et al*. (2012) evaluated a set of global and regional subduction ground motion models for their applicability to Peru-Chile. This evaluation utilized a recently compiled database of strong motion data form Peru and Chile. Using a maximum likelihood approach, Arango *et al*. (2012) favored, in order, the megathrust models of Zhao *et al*. (2006) followed by Youngs *et al*. (1997), and Atkinson and Boore (2003). We weighted the three models 0.4, 0.3, and 0.3, respectively in the PSHA.

For the intraslab model, Arango *et al*. (2012) rated the Zhao *et al*. (2006) model the highest followed by Atkinson and Boore (2003). We weighted these models at 0.55, and 0.45, respectively. The hazard was calculated for soil site conditions. A V_S30 of 310 m/sec was used in the NGA models. The subduction zone models are for generic soil.

6. RESULTS

The results of the PSHA for four cities for soil site conditions are presented in terms of ground motion as a function of annual exceedance probability. This probability is the reciprocal of the average return period. Figure 5 shows the mean hazard curves for peak horizontal ground acceleration (PGA). The PGA values for building code-relevant return periods of 475 and 2,475 years are listed in Table 2. This level of ground shaking can result in significant damage particularly for poorly designed and constructed buildings.

The contributions of the various seismic sources to the mean PGA hazard are also shown on Figure 5. The seismic sources that contribute to the PGA hazard varies by city but the crustal background seismicity within the coastal zone controls at short return periods (< 1,000 years). At longer return periods, the Colonche fault zone dominates the PGA hazard in Guayaquil (Figure 5a). In Manta and Salinas, it is the megathrust and in Machala, it is the intraslab seismicity. At longer spectral periods, e.g., 1.0 sec SA, the subduction zone controls the hazard because of its capability to generate greater long-period ground motions from the events of **M** 8 and greater.

Table 2. Mean Probabilistic PGA Values in g's

Cities	Return Period (years)	
	475	2,475
Guayaquil	0.41	0.70
Machala	0.39	0.61
Manta	0.35	0.65
Salinas	0.33	0.58

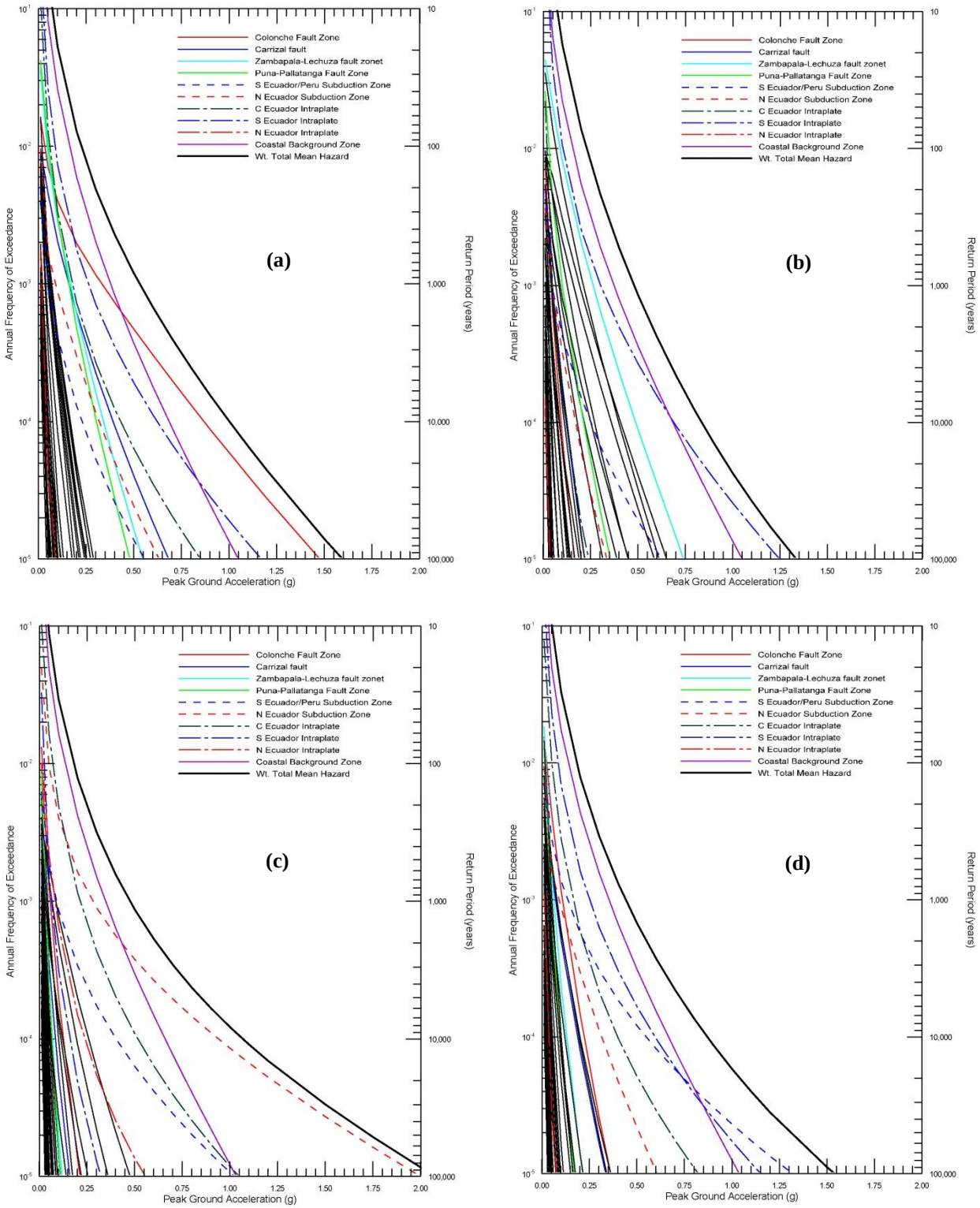

Figure 5. PGA hazard curves by seismic source: a) Guayaquil, b) Machala, c) Manta, d) Salinas

REFERENCES

Abrahamson, N.A. and Silva, W.J. (2008). Summary of the Abrahamson and Silva NGA ground motion relations. *Earthquake Spectra* **24**, 67-97.

Arango, M.C., Strasser, F.O., Bommer, J.J., Cepeda, J.M., Boroschek, R., Hernandez, D.A., and Tavera, H. (2012). An evaluation of the applicability of current ground-motion models to the South and Central American subduction zones. *Bulletin of the Seismological Society of America* **102**, 143-168.

Atkinson, G.M., and Boore, D.M. (2003). Empirical ground-motion relations for subduction zone earthquakes and their applications to Cascadia and other regions. *Bulletin of the Seismological Society of America* **93**, 1703-1729.

Boore, D.M. and Atkinson, G.M. (2008). Ground motion predictive equations for the average horizontal component of PGA, PGV, and 5% damped PSA at spectral periods between 0.01s to 10.0s. *Earthquake Spectra* **24**, 99-138.

Bourgois, J., Bigot-Cormier, F., Bourles, D., Braucher, R., Dauteuil, O., Witt, C., and Michaud, F. (2007). Tectonic record of strain buildup and abrupt coseismic stress release across the northwestern Peru coastal plain, shelf, and continental slope during the past 200 ky. *Journal of Geophysical Research* **112**, 22 p.

Bourgeois, J., Petroff, C., Yeh, H., Titov, V., Synolakis, C.E., Benson, B., Kuroiwa, J., Lander, J., and Norabuena, E. (1999). Geological setting, field survey and modeling of the Chimbote, Northern Peru, tsunami of 21 February 1996. *Pure and Applied Geophysics* **154**, 513-540.

Campbell, K.W. and Bozorgnia, Y. (2008). NGA ground motion model for the geometric mean horizontal component of PGA, PGV, PGD, and 5% damped linear elastic response spectra for periods ranging from 0.01 to 10s. *Earthquake Spectra* **24**, 139-171.

Chiou, B.S.J. and Youngs, R.R. (2008). An NGA model for the average horizontal component of peak ground motion and response spectra. *Earthquake Spectra* **24**, 173-215.

Cornell, C.A. (1968). Engineering seismic risk analysis. *Bulletin of the Seismological Society of America* **58**, 1583-1606.

Dumont, J.F., Santana, E., Vilema, W., Pedoja, K., Ordonez, M., Cruz, M., Jimenez, N., and Zambrano, I. (2005). Morphological and microtectonic analysis of Quaternary deformation from Puna and Santa Clara Islands, Gulf of Guayaquil, Ecuador (South America). *Tectonophysics* **399**, 331-350.

Eguez, A., Alvarado, A., Yepes, H., Machette, M.N., Costa, C.H., Dart, R.L., and Bradley, L.-A. (2003). Database and map of Quaternary faults and folds of Ecuador and its offshore regions. U.S. Geological Survey Open-File Report 03-289.

Gutscher, M.-A., Malavieille, J., Lallemand, S., and Collot, J.-Y. (1999). Tectonic segmentation of the North Andean margin: impact of the Carnegie Ridge collision. *Earth and Planetary Science Letters* **168**, 255–270.

Nishenko, S.P. (1991). Circum-Pacific seismic potential 1989-1999. *Pure and Applied Geophysics* **135**, 169-259.

Pelayo, A.M. and Wiens, D.A. (1990). The November 20, 1960 Peru tsunami earthquake: source mechanism of a slow event. *Geophysical Research Letters* **17**, 661-664.

Ruff, L. and Kanamori, H. (1983). Seismic coupling and uncoupling at subduction zones. *Tectonophysics* **99**, 99-117.

Weichert, D.H. (1980). Estimation of the earthquake recurrence parameters for unequal observation periods for different magnitude. *Bulletin of the Seismological Society of America* **70**, 1337-1346.

Wells, D.L. and Coppersmith, K.J. (1994). New empirical relationships among magnitude, rupture length, rupture width, rupture area, and surface displacement. *Bulletin of the Seismological Society of America* **84**, 974-1002.

Winter, T., Avouac, J.-P., and Lavenu, A. (1993). Late Quaternary kinematics of the Pallatanga strike-slip fault (central Ecuador) from topographic measurements of displaced morphological features. *Geophysical Journal International* **115**, 905-920.

Witt, C., Bourgois, J., François, M., Ordoñez, M., Jiménez, N., and Sosson, M. (2005). Development of the Golfo de Guayaquil (Ecuador) as an effect of the North Andean Block tectonic escape since the lower Pleistocene. *6th International Symposium on Andean Geodynamics*, Volume Extended Abstracts: Barcelona, Spain, 804-808.

Youngs, R.R., Chiou, S.-J, Silva, W.J., and Humphrey, J.R. (1997). Strong ground motion attenuation relationships for subduction zone earthquakes. *Seismological Research Letters* **68**, 58-73.

Zhao, J.X., Zhang, J., Asano, A., Ohno, Y., Oouchi, T., Takahashi, T., Ogawa, H., Irikura, K., Thio, H.K., Somerville, P.G., Fukushima,Y., and Fukushima, Y. (2006). Attenuation relations of strong ground motion in Japan using site classification based on predominant period. *Bulletin of the Seismological Society of America* **96**, 898-913.